Arab J Geosci (2016) 9:386
DOI 10.1007/s12517-016-2482-y

ORIGINAL PAPER

Simulation of temporal variation for reference evapotranspiration under arid climate

Amr Mossad [1,2] · **A. A. Alazba** [1,3]

Received: 26 August 2015 / Accepted: 22 April 2016

Abstract Reliable forecasting of evapotranspiration (ET) plays a critical role in the planning and management of water resources. Accordingly, this study aims to investigate the possibility of using autoregressive integrated moving average (ARIMA) models to anticipate monthly reference evapotranspiration (ET_o). Thus, a monthly ET_o time series of 34 years (1980–2014) is determined according to the FAO Penman-Monteith method. This time series is divided into two sets, which are used for developing and validating the ARIMA models. Subsequently, five tentative ARIMA models are created via the 19-year set (1980–1999). In order to reveal the best ARIMA structure among the developed models, the Akaike information criterion (AIC) and the Hannan-Quinn information criterion (HQC) are computed for comparison. The result of the comparison suggests that the ARIMA $(1,0,1) \times (0,1,1)_{12}$ model is strong enough to justify the goodness-of-fit requirements. Validation of the candidate ARIMA model is then conducted for the 15-year set (2000–2014). The validation result contends that there is a reasonable agreement between forecasted and observed time series with high coefficient of correlation (r = 0.966). Promisingly, it can be concluded that the candidate ARIMA model is capable of anticipating the monthly ET_o under arid climate.

✉ Amr Mossad
aabdelbary@ksu.edu.sa; amr_abdelbari@agr.asu.edu.eg

[1] Agricultural Engineering Department, King Saud University, Riyadh 11451, Kingdom of Saudi Arabia

[2] Agricultural Engineering Department, Ain Shams University, Cairo 11241, Egypt

[3] Alamoudi Water Research Chair, King Saud University, Riyadh 11451, Kingdom of Saudi Arabia

Keywords Hydrology · Climate change · Forecasting models · Time series · ARIMA

Introduction

Certainly, water is a scarce resource that will be an ever-increasing problem in the future. This is due to tremendous changes in the climate (Abu-Allaban et al. 2015). Such changes cause variations in air temperature, relative humidity, and solar radiation (Haskett et al. 2000) as well as they are expected to cause changes in the hydrological cycle by affecting precipitation and evapotranspiration (ET) (Yu et al. 2013). Therefore, any variations of the hydrological processes induced by climate change can be significantly reflected in ET (Chen et al. 2015; Zhang and Schilling 2006). The importance of ET in sustaining the hydrologic cycle and replenishing the world's freshwater resources is recognized (Katul and Novick 2009). For the practical purpose of water balance studies, there are three steps to evaluate the implications of climatic changes recommended by Gleick 1989. Firstly, develop the quantitative scenarios of changes in the major climatic variables, such as temperature, precipitation, and evapotranspiration. Secondly, simulate the hydrologic cycle for an area of interest, using the scenarios developed in the first step. Lastly, assess the implications of the hydrologic variations identified in the second step for performance of such water resource systems as dams, aqueducts, reservoirs, and groundwater recharge basins.

In this way, ET is one of the most important components of the hydrologic cycle. It integrates atmospheric and land surfaces, hydrology, and biological processes (Goyal 2004). The ET is an effective indicator for hydrologic systems (Huo et al. 2013) that consumes about 60–75 % of precipitation inputs (Zhou et al. 2008). Thus, the quantification of ET is crucial for

Published online: 27 April 2016

researchers interested in managing water (Jhorar et al. 2011), developing water-saving policies in irrigated areas (Qiu et al. 2015) and studying the impact of climate change on water resources (Bormann 2011). This insistent necessity of ET leads to extensive efforts and researches in the modeling of its mechanism. Consequently, many scientists have proposed and developed different methods for estimating the ET under different climatic conditions, including Penman (1948), Thornthwaite (1948), Makkink (1957), Turc (1961), and Priestley and Taylor (1972); most of these methods are described in Abtew and Melesse (2013). However, it is difficult to estimate the reference evapotranspiration (ET_o) in many areas due to the lack of adequate measurement of meteorological factors (Zhao et al. 2015). In the context of the lack of global validity of these methods, the Food and Agriculture Organization of the United Nations (FAO) adopted the FAO Penman-Monteith approach (FAO-56 PM) as the standard method for determining ET_o (Allen et al. 1998). This is also evidenced by a study conducted under hyper-arid environments (Alblewi et al. 2015).

The time series analysis is a theoretical explanation that allows the development of a mathematical model to explain systematic patterns embedded in the data. The most evident patterns appearing in time series data are trends and seasonality (Box and Jenkins 1976; Vandaele 1983). Additionally, the consequent time series observation depends on the previous one (Box et al. 2008). This dependency creates relationships between observations (Chen et al. 2009) and ensures that time series analysis is performed steadily (Roberts 2003). In the case of insufficient random processes (uncorrelated white noise) in the data, then it is hard to identify these patterns within the time series (Lange et al. 2013). Therefore, the abstracting of autocorrelation components from the data remains a challenge in time series analysis techniques (Sentas and Psilovikos 2010). Accordingly, monitoring, simulating, predicting, assessing, and managing can perform (Brockwell and Davis 2002). Recently, much effort has been dedicated to using the stochastic models in hydrology and climatology. One of the most extensively stochastic model used in analyzing hydrologic time series is the autoregressive integrated moving average (ARIMA) model. The recognition of ARIMA models in several areas is because of the flexibility and methodical searching at every step of the development (identifying, parameter estimating, and diagnostic checking) for an appropriate model (Yurekli et al. 2005; Zhang 2003). The forecasting using the ARIMA models has a favorable advantage due to their capability in detecting the time-associated changes in the series (Han et al. 2010).

Many scientists developed researches in light of the procedure proposed by Box and Jenkins 1976. Abebe and Foerch 2008 applied the Box and Jenkins methodology to identify a stochastic model that describes hydrologic drought. Landeras et al. 2009 forecasted weekly ET with autoregressive integrated moving average (ARIMA) and artificial neural network models. Kim et al. 2011 used the seasonal autoregressive moving average (SARIMA) model to evaluate and predict the temporal-spatial precipitation variability. Han et al. 2013 applied ARIMA modeling to drought forecasting using the standardized precipitation index (SPI). Mossad and Alazba 2015 predicted drought based on the standardized precipitation evapotranspiration index (SPEI). Meshram et al. 2015 modeled weather parameters using the SARIMA model as a viable tool for generating and forecasting of climatic parameters having inbuilt seasonal patterns. Hassan and Ansari 2015 performed a time series analysis of mean monthly river flow data. These attempts were useful and satisfactory in hydrologic forecasting in general. Accordingly, the main objective of the present study is to develop the stochastic models to forecast monthly ET_o under arid climate, in addition to the assessment of best-fitted ARIMA structure among the developed models in anticipating monthly ET_o time series.

Material and methods

Study area and dataset description

The study area has an arid-hot climate with high temperatures during the day and low temperatures at night. It has a very low average annual precipitation of 101.3 mm. The data pertaining to a meteorological station (24° 42′ 25.25″ N, 46° 43′ 7.23″ E, and 613 m above the sea level) located at the center of the city of Riyadh have been used in this study (Fig. 1).

Meteorological data were obtained from the Saudi Presidency of Meteorology and Environment (PME). The data of daily maximum and minimum temperatures, wind speed at the height of 2 m, precipitation, daily solar radiation, and relative humidity were used in developing the ET_o time series. This time series was created according to the calculation procedure given in FAO paper n. 56 (Allen et al. 1998). The period considered in this study for estimating ET_o was the years of 1980–2014. The ET_o equation can be expressed as follows:

$$ET_o = \frac{0.408\ \Delta\ (R_n - G) + \gamma\left(\frac{900}{T_a + 273}\right)U_2(e_s - e_a)}{\Delta + \gamma(1 + 0.3U_2)}$$

where ET_o is the reference evapotranspiration for clipped grass (mm day^{-1}), Δ the slop vapor of pressure curve (kPa °C^{-1}), R_n the net radiation at the crop surface (MJ m^{-2} day^{-1}), G the soil heat flux density (MJ m^{-2} day^{-1}), T the mean air temperature (°C), U_2 the wind speed at 2 m height (m s^{-1}), e_s the saturation vapor pressure (kPa), e_a the actual vapor pressure (kPa), and γ the psychrometric constant (kPa °C^{-1}).

Monthly values of the ET_o time series were divided into parts. The first part of the time series data, from 1980 to 1999,

Fig. 1 Map of the administrative areas of Saudi Arabia with the indication of the study region and location of meteorological station (*yellow star*)

was used to develop stochastic models. The total number of observations used in the model development was 240, with sampling intervals of 1 month and seasonality length of 12. Meanwhile, the second part of the time series data, from 2000 to 2014, was used to investigate the forecasting validity of the developed models. Table 1 contains the basic statistics of the monthly ET_o data. The results of basic statistics analysis revealed that both time series are homogenous and they do not vary from the whole data series.

Hydrologic time series concept

The hydrologic time series was described mathematically as a stochastic process. The ARIMA models are the most general and include many of the other models that describe this process. The multiplicative ARIMA is a combination of non-seasonal and seasonal models (Machiwal and Jha 2012; Maidment and Djokic 2000). The general form of the hydrologic time series was represented as follows:

Table 1 Main statistical parameters of the monthly reference evapotranspiration time series used in model development and validation

Parameters	Reference evapotranspiration time series		
	Whole data (1980–2014)	Model development (1980–2000)	Model validation (2001–2014)
Mean (mm)	217.32	232.98	224.03
No. of observations	420	240	180
Standard deviation (mm)	89.18	82.24	86.52
Skewness coefficient	0.20	−0.05	0.08
Kurtosis coefficient	−1.24	−1.23	−1.25

$$\varnothing(B)\Phi\left(B^S\right)\nabla^d\nabla_S^D Z_t = \theta(B)\Theta\left(B^S\right)e_t$$

where e_t is a normal independently distribution white noise residual series with mean zero and variance σ^2, B is the lag operator, Φ and Θ are the autoregressive and moving average coefficients, $\varnothing(B)$ is non-seasonal autoregressive of order p, and $\Phi(B^S)$ is the seasonal autoregressive operator of order P. The general forms of $\varnothing(B)$ and $\Phi(B^S)$ were introduced by the following equation:

$$\varnothing(B) = 1-\varnothing_1 B-\varnothing_2 B^2-\varnothing_2 B^2-\cdots\cdots-\varnothing_p B^p$$

$$\Phi\left(B^S\right) = 1-\Phi_1 B^s-\Phi_2 B^{2s}-\Phi_3 B^3-\cdots\cdots-\Phi_p B^p$$

where $\theta(B)$ is the non-seasonal moving average of order q and $\Theta(B^S)$ is the seasonal moving average of order Q. Both non-seasonal and seasonal parts were represented by

$$\theta(B) = 1-\theta_1 B-\theta_2 B^2-\theta_2 B^2-\cdots\cdots-\theta_q B^q$$

$$\Theta\left(B^S\right) = 1-\Theta_1 B^s-\Theta_2 B^{2s}-\Theta_3 B^{3s}-\cdots\cdots-\theta_Q B^{Qs}$$

Meanwhile, the ∇^d and ∇_S^D are the non-seasonal and seasonal differencing operators of order d and D, respectively; the S indicates the seasonality that equals to 12 for the monthly ET_o.

Results and discussion

Development of ARIMA model schemes

According to the methodology proposed by Box-Jenkins (1976), there are four steps used in developing the ET_o ARIMA model schemes. These steps are model identification, model estimation, diagnostic checking, and forecasting (Box and Jenkins 1976; Mishra and Desai 2005). In the following, there is a detailed explanation of each step.

Model identification

One of the basic concepts of the Box-Jenkins 1976 methodology when analyzing data is examining features of the time series such as trend and seasonality. This can be achieved through observing the original time series plots. The original time series of monthly ET_o data is shown in Fig. 2. This figure demonstrates an evident seasonal component in the original time series data, with repetition every 12 months. Therefore, the time series could be modeled.

In addition, Fig. 2 suggests that there are no abnormal flocculating trends in the data. The same thing is observed by inspection of autocorrelation (ACF) and partial autocorrelation functions (PACF) for the original data (Fig. 3a, b). These functions give more information on the behavior of the time series (Zhang 2003). However, the first differencing transformation of monthly ET_o was performed to create a stationary time series (Hyndman and Athanasopoulos 2014). The transformed monthly ET_o time series was then used as a new time series in developing the ARIMA models. After that, the ARIMA model structures suitable for a transformed data series were proposed. Hence, the ACF and PACF of the transformed data are plotted (Fig. 3c, d). Therefore, the possible combination of tentative ARIMA models that can be considered are ARIMA $(1,0,1) \times (0,1,1)_{12}$, ARIMA $(1,0,1) \times (0,1,2)_{12}$, ARIMA $(1,0,1) \times (1,1,1)_{12}$, ARIMA $(1,0,2) \times (0,1,1)_{12}$, and ARIMA $(1,0,1) \times (0,1,1)_{12}$ with constant.

Model estimation

In this step, the method of maximum likelihood was used in parameter estimation, as explained by Brockwell and Davis (2002). The most parsimonious model structure was selected through two information criteria. Thus, the Akaike information criterion (AIC) and Hannan-Quinn information criterion (HQC) were used. The model with the

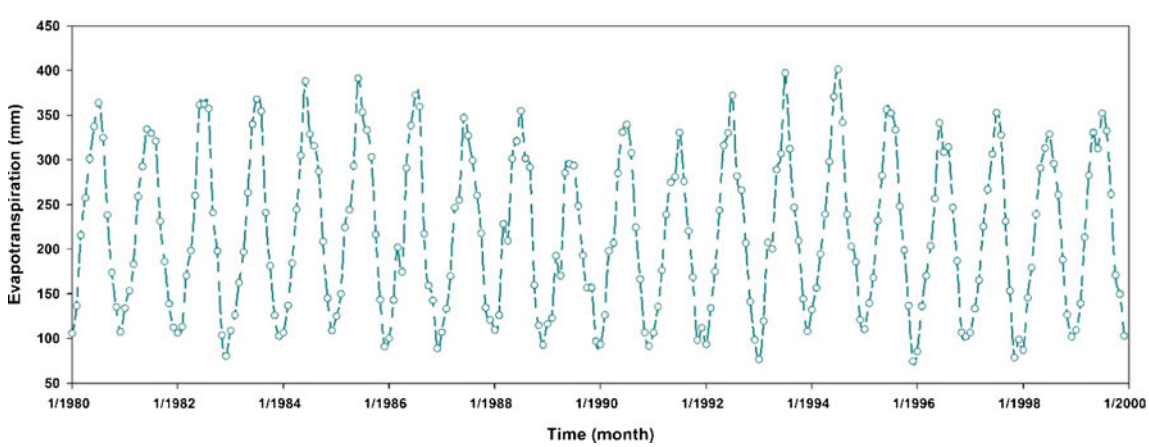

Fig. 2 Time series of observed monthly reference evapotranspiration over Riyadh region, Saudi Arabia, for the period 1980–2000

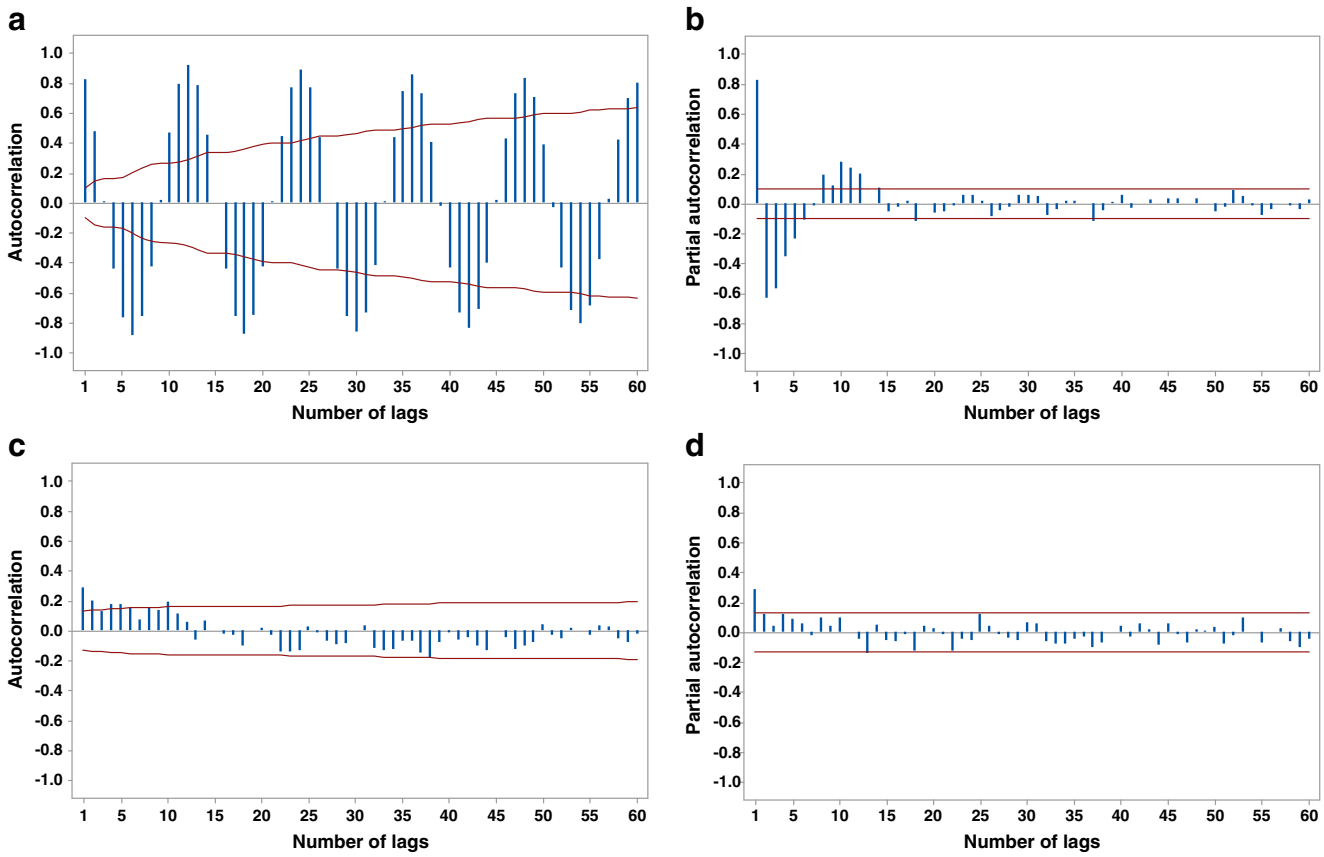

Fig. 3 Autocorrelation function (ACF) and partial autocorrelation function (PACF) patterns for original and differenced monthly ET_o time series; **a** ACF, **b** PACF, **c** transformed ACF, **d** transformed PACF

lowest AIC and HQC was selected as the best-fitted model (Marco et al. 2012). This is due to the model residuals being white noise (Tu and Xu 2012). Both criterions are defined mathematically as

$$\mathrm{AIC} = -2\log L + 2m$$

$$\mathrm{HQC} = -2L + 2m\log\log n$$

where L is the likelihood function of the ARIMA model, m is the number of terms estimated in the model, and n is the number of observations.

Table 2 Information criterion of tentative monthly ET ARIMA $(p, d, q) \times (P, D, Q)_S$ models

ARIMA model	Information criterion	
	AIC	HQC
ARIMA(1,0,1) × $(0,1,1)_{12}$	6.20657	6.2241
ARIMA(1,0,1) × $(0,1,2)_{12}$	6.21457	6.23795
ARIMA(1,0,1) × $(1,1,1)_{12}$	6.21517	6.23855
ARIMA(1,0,2) × $(0,1,1)_{12}$	6.21852	6.24083
ARIMA(1,0,1) × $(0,1,1)_{12}$ with constant	6.21916	6.24178

Based on the results shown in Table 2, the ARIMA (1,0,1) × $(0,1,1)_{12}$ model was identified as the best-fitted model with minimum information criteria (AIC and HQC). The smallest AIC value has residuals, which resemble white noise (Mishra and Desai 2005). However, this confirms the appropriateness of the selected ARIMA model (Brockwell and Davis 2002).

AIC Akaike information criterion, *HQC* Hannan-Quinn information criterion

After selecting the best-fitted ARIMA model, the estimated values of different model terms (AR, MA, and SMA) were studied. Table 3 summarizes the statistical significance of the terms in the selected ARIMA model.

Table 3 Summary of statistical analysis of the candidate monthly ET ARIMA (1, 0, 1) $(0, 1, 1)_{12}$ model

Model parameter	Estimate value	Standard error	*t* ratio	*p* value
AR(1)	0.87756	0.0732557	11.9794	0.000000
MA(1)	0.690231	0.107924	6.39551	0.000000
SMA(1)	0.917403	0.0163338	56.166	0.000000

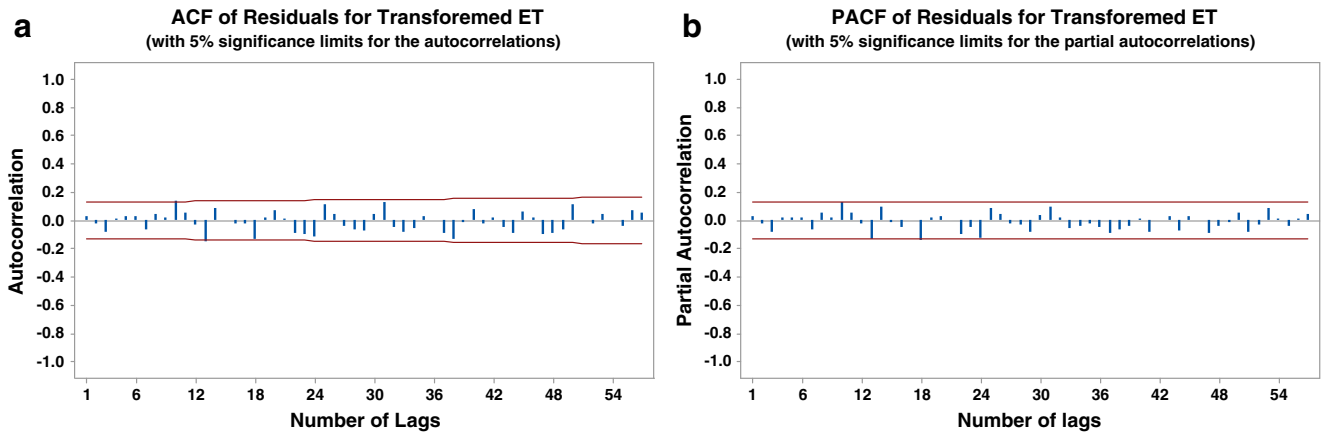

Fig. 4 Autocorrelation function (*ACF*) and partial autocorrelation function (*PACF*) of residuals for the candidate ARIMA model with 5 % significance limits

All ARIMA model terms have p values less than 0.05. Therefore, these terms are statistically significantly different from zero at the 95.0 % confidence level. The p values of AR(1), MA(1), and SMA(1) are less than 0.05, so they are significantly different from 0. The estimated standard deviation of the input white noise equals 22.2361.

Diagnostic checking

After fitting the ARIMA model, the result of the candidate ARIMA model needed to be validated. It is a very important and last step before using the candidate model in forecasting. This step assures the reliability and acceptability of the candidate model. The graphical technique is a convenient method

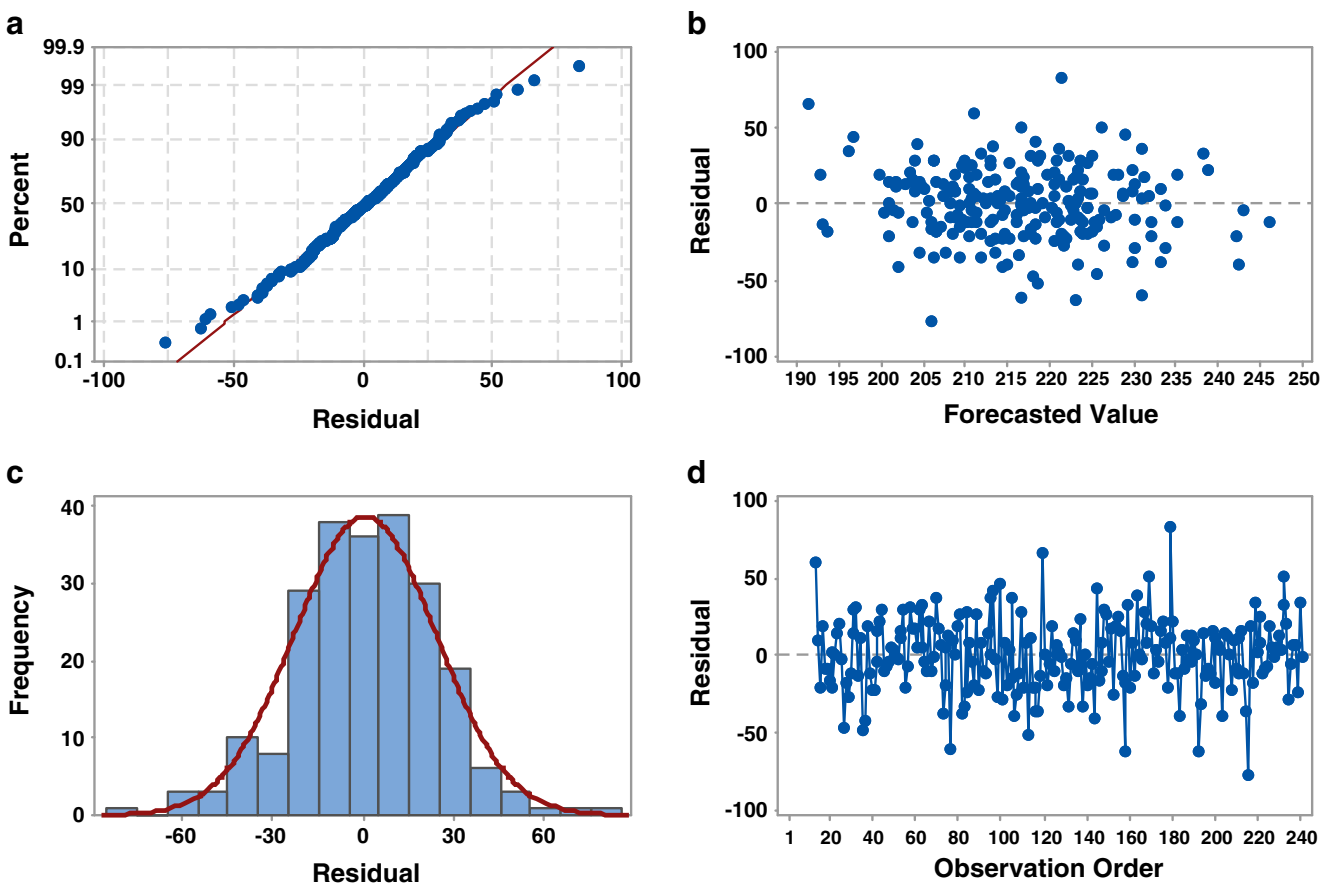

Fig 5 Residual plots for the candidate ARIMA model

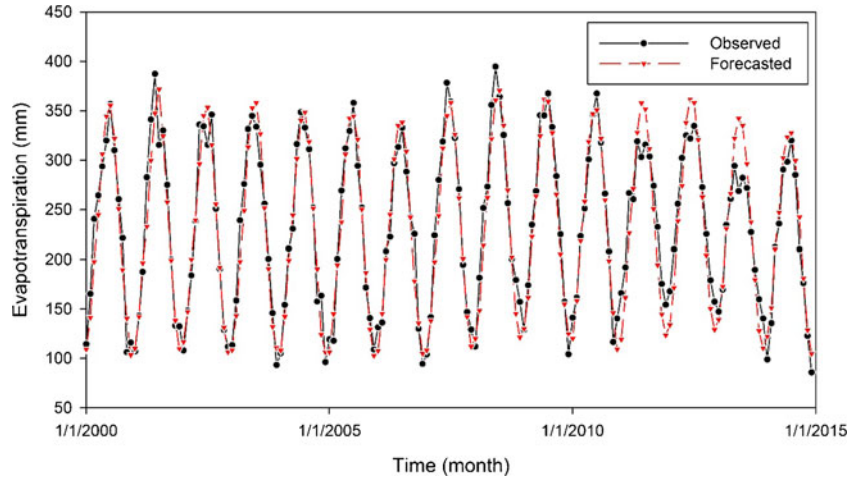

Fig 6 Time plot comparison between observed monthly ET_o and forecasted ET_o using the best-fitted ARIMA (1,0,1) × $(0,1,1)_{12}$ model (validation period, 2000–2014)

that validates the model. It tests the assumptions for the residuals. Hence, many validation plots are investigated to check if the residuals correlate to white noise or not. These plots can be summarized as follows: ACF and PACF of residuals, histogram of residuals, normal probability of residuals, and residuals vis-à-vis forecasted values.

Figure 4a, b depicts the estimated ACF and PACF of residuals for the candidate model at various numbers of lags with 95 % probability. As noted, most of the ACF and PACF values are not significantly different from zero within confidence limits. Therefore, no significant correlation was found between residuals.

Additionally, residual plots in Fig. 5 examine the adequacy of the candidate ARIMA (1,0,1) × $(0,1,1)_{12}$ model. Figure 5a appeared as a straight line for the residual; this was likely due to the normality assumptions of the residuals. Only a few points were lying away from the straight line, which implied a distribution with outliers. The histogram of the residuals shown in Fig. 5b follows the normal distribution that signifies residuals to be white noise. Figure 5c demonstrates that the residual values are normally distributed around the mean. Likewise, Fig. 5d shows the residual values of the differences between the observed and forecasted values at different observation orders. These values are fluctuating around zero, which indicates the goodness of fit of the candidate ARIMA model.

Table 4 Comparison of the basic statistical properties of the data used in the validation and forecasted data from the best-fitted ARIMA model

	Observed	Forecasted
Mean	232.983	229.733
Variance	6762.828	7433.660
Observations	180	180
$F_{calculated} < F_{critical\ one\text{-}tail}$	1.099 < 1.280	
$\lvert Z_{calculated}\rvert < Z_{critical\ two\ tail}$	0.366 < 1.960	

Forecasting using the candidate ARIMA model

The forecasting was done at a lead time of 1-month using the candidate ARIMA (1,0,1) × $(0,1,1)_{12}$ model. The monthly ET_o time series from 2000 to 2014 was used to compare the observed and forecasted values. The relationship between the observed and forecasted data using the selected ARIMA (1,0,1) × $(0,1,1)_{12}$ model is shown in Fig. 6. The comparison of the basic statistical properties of the observed and forecasted time series is presented in Table 4. The $Z_{calculated}$ value of the mean was less than $Z_{critical}$ tabular values (±1.96 for two tails at a significance level of 5 %). Similarly, the $F_{calculated}$ value of standard deviation was less than $F_{critical}$ tabular value (±1.280 for one tail at a significance level of 5 %). Therefore, there is no significant difference between the mean and standard deviation values of the observed and forecasted data. Figure 7 confirms this good agreement correlation between the observed and forecasted data with Pearson's $r = 0.966$.

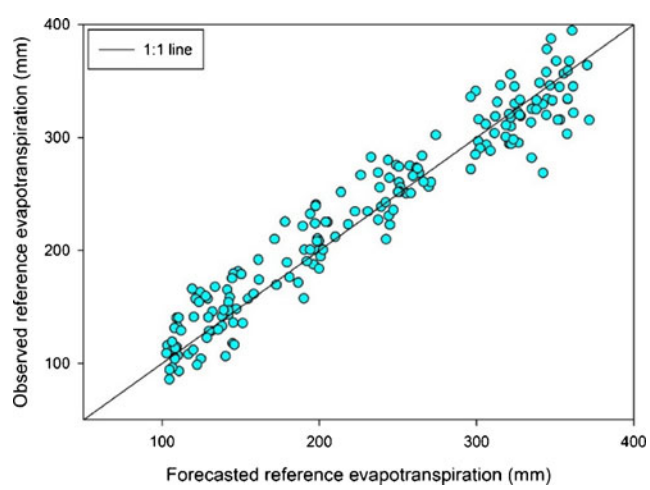

Fig. 7 Dispersion diagram of observed monthly ET_o versus forecasted monthly ET_o using the best-fitted ARIMA (1,0,1) × $(0,1,1)_{12}$ model (validation period, 2000–2014)

Conclusions

The forecasting of ET in hyper-arid climates contributes to our understanding of what is likely to continue and what could possibly change in the hydrologic cycle. Therefore, this study focused on the possibility of forecasting the monthly reference evapotranspiration (ET_o) using the Box-Jenkins (1976) methodology of stochastic modeling. Accordingly, five ARIMA model structures have been proposed using different correlation methods (ACF and PACF). The best ARIMA model structure was selected according to the information criteria (AIC and HQC). The most parsimonious ARIMA model that has a lower value of AIC and HQC is an ARIMA (1,0,1) × $(0,1,1)_{12}$ model. All candidate ARIMA model terms (AR(1), MA(1), and SMA(1)) had p values less than 0.05, which were significantly different from zero. Hence, this ARIMA model structure was used to generate a forecasted time series. There was no statistical difference between the observed and forecasted monthly ET_o time series. Moreover, the coefficient of correlation between both the observed and the forecasted time series was high. These results are promising, and the proposed ARIMA model structure could be considered for forecasting of monthly ET_o time series under arid conditions.

Acknowledgments The project was financially supported by King Saud University, Vice Deanship of Research Chairs.

References

Abebe A, Foerch G (2008) Stochastic simulation of the severity of hydrological drought. Water and Environment Journal 22:2–10

Abtew W, Melesse A (2013) Evaporation and evapotranspiration: measurements and estimations. Springer Science & Business Media, p. 206

Abu-Allaban M, El-Naqa A, Jaber M, Hammouri N (2015) Water scarcity impact of climate change in semi-arid regions: a case study in Mujib basin. Jordan Arab J Geosci 8:951–959

Alblewi B, Gharabaghi B, Alazba AA, Mahboubi A (2015) Evapotranspiration models assessment under hyper-arid environment. Arab J Geosci 8:9905–9912

Allen RG, Pereira LS, Raes D, Smith M (1998) Crop evapotranspiration: guidelines for computing crop water requirements. vol FAO Irrigation and Drainage Papers (Book 56). Food and Agriculture Organization of the United Nations, Rome, pp. pp 17–pp 27

Bormann H (2011) Sensitivity analysis of 18 different potential evapotranspiration models to observed climatic change at German climate stations. Climatic Change 104:729–753

Box GEP, Jenkins GM (1976) Time series analysis: forecasting and control. Holden-Day, pp 575

Box GEP, Jenkins GM, Reinsel GC (2008) Time series analysis: forecasting and control. Wiley, pp 784

Brockwell PJ, Davis RA (2002) Introduction to time series and forecasting. 2 edn. Springer, New York, p. 437

Chen CF, Chang YH, Chang YW (2009) Seasonal ARIMA forecasting of inbound air travel arrivals to Taiwan. Transportmetrica 5:125–140

Chen X, Liu X, Zhou G, Han L, Liu W, Liao J (2015) 50-year evapotranspiration declining and potential causations in subtropical Guangdong province, southern China. Catena 128:185–194

Gleick PH (1989) Climate change, hydrology, and water resources. Rev Geophys 27:329–344

Goyal RK (2004) Sensitivity of evapotranspiration to global warming: a case study of arid zone of Rajasthan (India). Agric Water Manag 69: 1–11

Han P, Wang PX, Zhang SY, Zhu DH (2010) Drought forecasting based on the remote sensing data using ARIMA models. Math Comput Model 51:1398–1403

Han P, Wang P, Tian M, Zhang S, Liu J, Zhu D (2013) Application of the ARIMA models in drought forecasting using the standardized precipitation index. In: Li D, Chen Y (eds) Computer and computing technologies in agriculture VI, IFIP Advances in Information and Communication Technology, vol 392. Springer, Berlin Heidelberg, pp. 352–358

Haskett JD, Pachepsky YA, Acock B (2000) Effect of climate and atmospheric change on soybean water stress: a study of Iowa. Ecological Modelling 135:265–277

Hassan S, Ansari MR (2015) Hydro-climatic aspects of Indus River flow propagation. Arab J Geosci 8:10977–10982

Huo Z, Dai X, Feng S, Kang S, Huang G (2013) Effect of climate change on reference evapotranspiration and aridity index in arid region of China. J Hydrol 492:24–34

Hyndman RJ, Athanasopoulos G (2014) Forecasting: principles and practice. OTexts, pp 291

Jhorar RK, Smit AAMFR, Bastiaanssen WGM, Roest CWJ (2011) Calibration of a distributed irrigation water management model using remotely sensed evapotranspiration rates and groundwater heads. Irrig Drain 60:57–69

Katul G, Novick K (2009) Evapotranspiration. In: Likens GE (ed) Encyclopedia of inland waters. Academic Press, Oxford, pp. 661–667

Kim B, Hossein S, Choi G (2011) Evaluation of temporal-spatial precipitation variability and prediction using seasonal ARIMA model in Mongolia. KSCE J Civ Eng 15:917–925

Landeras G, Ortiz-Barredo A, López J (2009) Forecasting Weekly Evapotranspiration with ARIMA and Artificial Neural Network Models. J Irrig Drain Eng 135:323–334

Lange H, Rosso OA, Hauhs M (2013) Ordinal pattern and statistical complexity analysis of daily stream flow time series. Eur Phys J Spec Top 222:535–552

Machiwal D, Jha MK (2012) Hydrologic time series analysis: theory and practice. Springer Science & Business Media, pp 280

Maidment DR, Djokic D (2000) Hydrologic and hydraulic modeling support: with geographic information systems. ESRI Press, pp 232

Makkink GF (1957) Testing the Penman formula by lysimeter. J Int Water Eng 11(3):277–288

Marco JB, Harboe R, Salas JD (2012) Stochastic hydrology and its use in water resources systems simulation and optimization. Springer, Netherlands, p. 483

Meshram D, Jadhav VT, Gorantiwar SD, Chandra R (2015) Modeling of weather parameters using stochastic methods. In: Singh AK, Dagar JC, Arunachalam A,R,G, Shelat KN (eds) Climate change modelling, planning and policy for agriculture. Springer, India, pp. 67–77

Mishra AK, Desai VR (2005) Drought forecasting using stochastic models. Stoch Environ Res Ris Assess 19:326–339

Mossad A, Alazba AA (2015) Drought Forecasting Using Stochastic Models in a Hyper-Arid Climate. Atmosphere 6:410–430

Penman HL (1948) Natural Evaporation from Open Water, Bare Soil and Grass. Proc., Royal Soc., London 193:120–145

Priestley CHB, Taylor RJ (1972) On the assessment of surface heat flux and evaporation using largescale parameters. Mon Weather Rev 100:81–92

Qiu R, Du T, Kang S, Chen R, Wu L (2015) Assessing the SIMDualKc model for estimating evapotranspiration of hot pepper grown in a solar greenhouse in Northwest China. Agric Syst 138:1–9

Roberts S (2003) Combining data from multiple monitors in air pollution mortality time series studies. Atmos Environ 37:3317–3322

Sentas A, Psilovikos A (2010) Comparison of ARIMA and transfer function (TF) models in water temperature simulation in dam–lake Thesaurus, eastern Macedonia, Greece. In: Environmental Hydraulics, Two Volume Set. CRC Press, pp 929–934

Thornthwaite CW (1948) An approach toward a rational classification of climate. Geogr Rev 38:55–94

Tu S, Xu L (2012) A theoretical investigation of several model selection criteria for dimensionality reduction. Pattern Recogn Lett 33: 1117–1126

Turc L (1961) Estimation of Irrigation Water Requirements, Potential Evapotranspiration: A Simple Climatic Formula Evolved Up to Date. Ann. Agronomy 12:13–49

Vandaele W (1983) Applied time series and Box-Jenkins models. Academic Press, pp 417

Yu L, Xia Z, Li J, Cai T (2013) Climate change characteristics of Amur River. Water Sci Eng 6:131–144

Yurekli K, Kurunc A, Ozturk F (2005) Application of linear stochastic models to monthly flow data of Kelkit Stream. Ecol Model 183:67–75

Zhang GP (2003) Time series forecasting using a hybrid ARIMA and neural network model. Neurocomputing 50:159–175

Zhang YK, Schilling KE (2006) Effects of land cover on water table, soil moisture, evapotranspiration, and groundwater recharge: a Field observation and analysis. J Hydrol 319:328–338

Zhao S-h et al. (2015) Rapid evaluation of reference evapotranspiration in Northern China. Arab J Geosci 8:647–657

Zhou G, Sun G, Wang X, Zhou C, McNulty SG, Vose JM, Amatya DM (2008) Estimating forest ecosystem evapotranspiration at multiple temporal scales with a dimension analysis Approach1 JAWRA. J Am Water Resour Assoc 44:208–221